Phase Relations in the Systems Na_2O–IrO_2 and Na_2O–PtO_2 in Air

C. L. McDANIEL

National Bureau of Standards, Washington, D.C. 20234

The equilibrium phase relations for the Na_2O–IrO_2 and Na_2O–PtO_2 systems were determined in air using the quenching technique. The Na_2O–IrO_2 system contains two stable compounds $Na_2O \cdot IrO_2$ and $2Na_2O \cdot 3IrO_2$, which dissociate at 1235 and 1040°C, respectively. The Na_2O–PtO_2 system contains three compounds: $Na_2O \cdot PtO_2$, metastable $2Na_2O \cdot 3PtO_2$, and $Na_xPt_3O_4$ ($0 \leqslant x \leqslant 1$). Their dissociation temperatures are 890, 710, and 810°C, respectively. Indexed X-ray diffraction powder patterns for $Na_2O \cdot IrO_2$ and $2Na_2O \cdot 3IrO_2$ are given.

1. Introduction

This study is part of a general program of phase equilibrium investigations involving the alkaline earth and alkali metal oxides with the Pt-group metal oxides (*1–3*). These systems have practical importance since Pt-group metals are used extensively in metal–oxide studies, for container materials and other high-temperature applications. Equilibrium relationships of the condensed phases in the Na_2O–IrO_2 and Na_2O–PtO_2 systems in air are presented here.

2. Experimental Procedure

Specimens were prepared from 0.3 g batches of various combinations of sodium carbonate and IrO_2 or Pt powder (Pt black), each having a purity of at least 99.8%. Calculated amounts of each end member, corrected for ignition loss, were weighed to the nearest milligram. Each batch was thoroughly hand mixed and a portion was heated at the temperature of interest. Specimen containers were gold or platinum tubes; no apparent reaction occurred with the various oxide samples. Experiments were conducted in a platinum alloy wire-wound quench furnace at various temperatures for different periods of time, and quenched in air. Temperatures in the quench furnace were measured with a Pt–Pt, 10% Rh calibrated thermocouple. All furnace temperatures[1] are considered accurate

to ±5°C. The precision of the measurements was estimated to be ±2°C.

The stability of a compound was established by heating first above and then below the dissociation temperature. Stable compounds reformed from the dissociation products; if prolonged heating failed to reform the phase, it was assumed to be metastable, forming only when heating the starting materials. All specimens were examined by X-ray diffraction at room temperature with a high-angle-recording Geiger counter diffractometer and Ni-filtered Cu radiation ($\lambda = 1.54056$ Å). The scanning rate was $1/4°$ 2θ/min. Unit cell dimensions were refined by a least-squares computer program[2] and estimated accurate to at least 2 in the last decimal place.

3. Results and Discussion

3.1. Na_2O–IrO_2 System

The phase diagram for the Na_2O–IrO_2 system in air is given in Fig. 1. The diagram was constructed from the data listed in Table I. It should be emphasized that Fig. 1 does not represent a true binary system. The portion between 50 to 100 mole % IrO_2 represents a composite of the Na_2O–IrO_2 and Na_2O–Ir systems in the Na–Ir–O_2 ternary. As the temperature is increased, the solid phases decompose by apparent oxygen loss.

[2] H. T. Evans, Jr., D. E. Appleman, and D. S. Handwerker, Amer. Crystal. Ass. Annu. Meet., Cambridge, MA, Program 43-43 (1963).
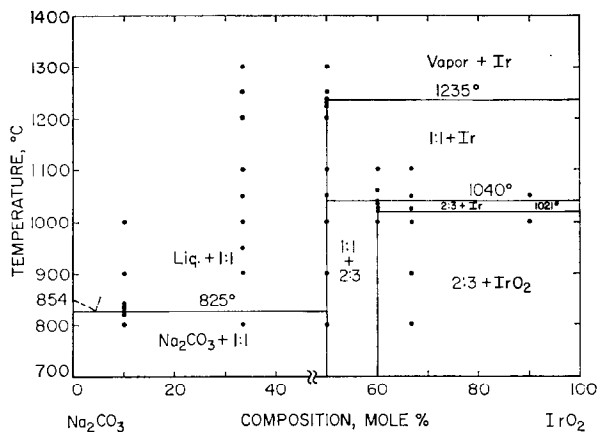
[1] All temperatures listed in this paper apply to the IPTS 1968.

FIG. 1. Phase diagram for the $Na_2O–IrO_2$ system in air. (●) Compositions and temperatures of experiments conducted. $(1:1) Na_2O \cdot IrO_2$, $(2:3) 2Na_2O \cdot 3IrO_2$. Polymorphic phase transformations in Na_2CO_3 (5), were not investigated nor indicated on diagram. Break in base line indicates two systems $Na_2CO_3–Na_2O \cdot IrO_2$ and $Na_2O \cdot IrO_2–IrO_2$.

Illustrating a dissociation as a type of phase transition or decomposition in which the vapor phase is ignored gives a simple binary representation of the ternary phase relations. This method of representation has been used by other investigators and is discussed in detail (1, 4). The portion of the diagram between 0 to 50 mole % IrO_2 represents the system $Na_2CO_3–Na_2O \cdot IrO_2$.[3] It is not known whether $Na_2CO_3–Na_2O \cdot IrO_2$ is a true binary system, as the system contains liquid of undetermined composition.

Resiman (5) reported the melting point for Na_2CO_3 as 854°C. The present work is in good agreement. There is a "eutectic" on the Na_2CO_3-rich side of the diagram. Polymorphic phase transformations in Na_2CO_3 reported by Reisman (5) were not investigated in this study nor indicated on the diagrams. Table II lists the X-ray powder pattern for the $Na_2O \cdot IrO_2$ (1:1) compound indexed on the basis of a monoclinic cell, space group $C2/c$, with $a = 5.418$ Å, $b = 9.394$ Å, $c = 10.765$ Å, and $\beta = 99°35'$. The room temperature X-ray pattern was obtained from a specimen equilibrated at 800°C and quenched in air. The dissociation temperature was established as 1235°C. Specimens heated above 1235°C gave X-ray diffraction patterns indicating only Ir metal present. It is assumed vapor (Na_2O and/or Na_2CO_3) and Ir metal are the equilibrium phases at these temperatures.

[3] Designations, such as $Na_2O \cdot IrO_2$ and Na_2IrO_3, are used interchangeably.

Scheer, VanArkel and Heyding (6) reported that the $Na_2O \cdot IrO_2$ phase is isomorphous with the A_2BO_3 series of compounds proposed by Lang (7). The series includes, among others, the $Li_2O \cdot TiO_2$ and $Na_2O \cdot SnO_2$ compound which were described by reference to a monoclinic cell, as well as to a larger orthorhombic cell, three times the volume of the former. Scheer, VanArkel and Heyding (6) reported the parameters of both cells for the $Na_2O \cdot IrO_2$ phase but the exact symmetry was left undecided. The indexed powder pattern is inaccurately described by Scheer, VanArkel and Heyding (6), although the monoclinic cell dimensions are in agreement with the parameters obtained in the present study. The structure of the $Li_2O \cdot TiO_2$ phase has since been reported by Dorrian and Newnham (8) based on single crystal data which indicated that the phase has monoclinic symmetry. X-Ray powder patterns of $Na_2O \cdot IrO_2$ and $Li_2O \cdot TiO_2$ obtained in this study, indicate the phases are similar in structure.

The $Na_2O \cdot IrO_2$ compound is a black powder which is reasonably stable at room temperatures but decomposes slowly over a period of several months in an air environment. Hydrolysis of the 1:1 compound was detected when in contact with water. The specimen was placed in water and dried at 100°C. Additional broad X-ray lines were observed at temperatures up to 200°C.

Unit cell dimensions and weight change versus temperature for the 1:1 compound are given in

Table I. Experimental Data for Compositions in the Na_2O-IrO_2 System

Composition		Heat Treatment[a]	X-ray Diffraction Analyses[b]	Remarks
Na_2O	IrO_2	Temp. Time		
Mol%	Mol%	°C-hr		
90	10	800-18	Na_2CO_3+$Na_2O\cdot IrO_2$	
		820-1/2		solid
		825-1/2		solid + liquid
		830-1/2	Na_2CO_3+$Na_2O\cdot IrO_2$	solid + liquid
		835-1/2		solid + liquid
		840-1/2		solid + liquid
		900-20	Na_2CO_3+$Na_2O\cdot IrO_2$	
		1000-62	$Na_2O\cdot IrO_2$	Na_2CO_3 volatilized
66.6	33.3	800-41	$Na_2O\cdot IrO_2$+Na_2CO_3	
		900-19	$Na_2O\cdot IrO_2$+Na_2CO_3	
		950-1[c]	IrO_2+Na_2CO_3+$Na_2O\cdot IrO_2$	trace amount of $Na_2O\cdot IrO_2$
		1000-20	$Na_2O\cdot IrO_2$+Na_2CO_3	
		1000-23	$Na_2O\cdot IrO_2$+Na_2CO_3	
		1050-4	$Na_2O\cdot IrO_2$+Na_2CO_3	
		1050-19	$Na_2O\cdot IrO_2$	Na_2CO_3 volatilized
		1100-2	$Na_2O\cdot IrO_2$+Na_2CO_3	quenched in liquid nitrogen
		1100-65	$Na_2O\cdot IrO_2$	Na_2CO_3 volatilized
		1200-2	$Na_2O\cdot IrO_2$	quenched in liquid nitrogen
		1200-21[c]	$Na_2O\cdot IrO_2$+Na_2CO_3	previous heat treatment 1050-4
		1250-19[c]	$Na_2O\cdot IrO_2$+Na_2CO_3	previous heat treatment 1000-1
		1300-24[c]	$Na_2O\cdot IrO_2$+Na_2CO_3	previous heat treatment 1000-2
50	50	700-120	$Na_2O\cdot IrO_2$	
		800-21	$Na_2O\cdot IrO_2$	
		900-20	$Na_2O\cdot IrO_2$	
		1000-2	$Na_2O\cdot IrO_2$	
		1000-15	$Na_2O\cdot IrO_2$	slow cooled 1°/min
		1000-22	$Na_2O\cdot IrO_2$	
		1050-21	$Na_2O\cdot IrO_2$	
		1100-2	$Na_2O\cdot IrO_2$	quenched in liquid nitrogen
		1100-66	$Na_2O\cdot IrO_2$	
		1200-2	$Na_2O\cdot IrO_2$	quenched in liquid nitrogen
		1200-2	$Na_2O\cdot IrO_2$	
		1225-2	$Na_2O\cdot IrO_2$	
		1230-2	$Na_2O\cdot IrO_2$	
		1235-2	$Na_2O\cdot IrO_2$+Ir	dissociation temperature
		1250-2	Ir	
		1250-19[c]	$Na_2O\cdot IrO_2$	previous heat treatment 1000-1
		1300-2	Ir	
40	60	1000-22	$2Na_2O\cdot 3IrO_2$+$Na_2O\cdot IrO_2$+IrO_2	nonequilibrium
		1000-68	$2Na_2O\cdot 3IrO_2$+$Na_2O\cdot IrO_2$+IrO_2	nonequilibrium
		1000-72	$2Na_2O\cdot 3IrO_2$+$Na_2O\cdot IrO_2$	previous heat treatment 1100-2
		1025-20	$2Na_2O\cdot 3IrO_2$+$Na_2O\cdot IrO_2$+Ir	nonequilibrium
		1030-2	$2Na_2O\cdot 3IrO_2$+$Na_2O\cdot IrO_2$	
		1035-2	$2Na_2O\cdot 3IrO_2$+$Na_2O\cdot IrO_2$	
		1040-2	$Na_2O\cdot IrO_2$+Ir	dissociation temperature
		1040-18	$Na_2O\cdot IrO_2$+Ir	
		1060-2	$Na_2O\cdot IrO_2$+Ir	
		1100-2	$Na_2O\cdot IrO_2$+Ir	
33.3	66.6	800-41	$2Na_2O\cdot 3IrO_2$+IrO_2+$Na_2O\cdot IrO_2$	nonequilibrium
		900-19	$2Na_2O\cdot 3IrO_2$+IrO_2+$Na_2O\cdot IrO_2$	trace amount of $Na_2O\cdot IrO_2$
		1000-23	$2Na_2O\cdot 3IrO_2$+IrO_2+$Na_2O\cdot IrO_2$	nonequilibrium
		1000-64	$2Na_2O\cdot 3IrO_2$+IrO_2+$Na_2O\cdot IrO_2$	previous heat treatment 1000-23
		1025-20	$2Na_2O\cdot 3IrO_2$+Ir+$Na_2O\cdot IrO_2$	quenched in liquid nitrogen
		1050-19	$Na_2O\cdot IrO_2$+Ir	
		1100-66	Ir+$Na_2O\cdot IrO_2$	
10	90	1000-20	IrO_2+$2Na_2CO_3\cdot 3IrO_2$	
		1040-46	Ir	Na_2CO_3 volatilized
		1050-2	Ir+$2Na_2CO_3\cdot 3IrO_2$+$Na_2CO_3\cdot IrO_2$	nonequilibrium

[a] All specimens were heat treated in open gold or platinum tubes and air quenched unless otherwise indicated. All temperatures listed applied to (IPTS 1968).

[b] Phases identified are given in order of the relative amount present at room temperature.

[c] Sealed platinum tube container; quenched in ice water.

Table II.   X-ray Diffraction Powder Data for $Na_2O \cdot IrO_2$ and $2Na_2O \cdot 3IrO_2$
(CuKα radiation)[a]

$Na_2O \cdot IrO_2$ [b]

hkℓ	d(Å) obs	d(Å) calc	I/I_1
002	5.313	5.307	100
020	4.696	4.697	15
$\bar{1}$11	4.505	4.501	10
111	4.051	4.045	7
022	3.517	3.517	4
$\bar{1}$13	3.031	3.034	3
131 ⎫ 200 ⎭	2.672	2.672 ⎫ 2.671 ⎭	56
004	2.653	2.654	33
131 ⎫ $\bar{2}$02 ⎭	2.566	2.567 ⎫ 2.564 ⎭	63
040 ⎫ 221 ⎭	2.344	2.349 ⎫ 2.340 ⎭	2
220	2.322	2.322	3
202 ⎫ $\bar{1}$33 ⎭	2.241	2.241 ⎫ 2.240 ⎭	85
133	2.065	2.065	15
006	1.7689	1.7691	6
204	1.7428	1.7432	14
135	1.6055	1.6049	15
060	1.5657	1.5657	19
062	1.5017	1.5017	12
206	1.3737	1.3735	4
064	1.3486	1.3485	11
262 ⎫ $\bar{4}$00 ⎭	1.3361	1.3362 ⎫ 1.3357 ⎭	5
$\bar{2}$62	1.2835	1.2835	7
402 ⎫ 264 ⎭	1.2469	1.2471 ⎫ 1.2470 ⎭	3
335 ⎫ 441 ⎭	1.1728	1.1727 ⎫ 1.1726 ⎭	3
404	1.1204	1.1205	3
355 ⎫ 139 ⎭	1.0490	1.0491 ⎫ 1.0490 ⎭	1
$\bar{5}$32	1.0233	1.0234	3
531	0.9920	0.9920	4
193	0.9758	0.9757	2
2,0,10	0.9345	0.9345	2
427	0.9109	0.9109	3
$\bar{3}$91	0.9038	0.9037	3
391	0.8910	0.8910	2

$2Na_2O \cdot 3IrO_2$ [c]

hkℓ	d(Å) obs	d(Å) calc	I/I_1
110	6.35	6.35	42
111	5.190	5.188	100
210	4.017	4.018	34
211	3.667	3.668	10
300	2.996	2.995	3
310	2.841	2.841	3
311	2.707	2.709	69
222	2.592	2.594	72
320	2.491	2.492	6
321	2.401	2.401	9
400	2.245	2.246	67
322	2.179	2.179	6
330	2.117	2.118	5
331	2.061	2.061	22
421	1.960	1.961	9
332	1.9156	1.9157	5
430	1.7968	1.7970	2
510	1.7621	1.7621	8
511	1.7293	1.7292	20
520	1.6682	1.6685	5
440	1.5886	1.5884	32
522	1.5635	1.5641	3
530	1.5410	1.5410	2
531	1.5186	1.5188	15
600	1.4973	1.4975	1
610	1.4767	1.4771	1
611	1.4574	1.4576	1
621	1.4035	1.4033	3
541	1.3868	1.3865	4
533	1.3701	1.3702	5
622	1.3548	1.3546	16
630	1.3396	1.3394	2
444	1.2971	1.2969	6
550	1.2709	1.2707	2
551	1.2585	1.2582	5
720	1.2345	1.2342	2
721	1.2231	1.2227	2
731	1.1699	1.1698	5
650	1.1505	1.1504	1
651	1.1412	1.1411	2
800	1.1233	1.1232	3
751	1.0376	1.0375	3
662	1.0308	1.0307	5
840	1.0048	1.0046	5
911	0.9863	0.9863	3
844	0.9171	0.9171	4

[a] d - interplanar spacing, I/I_1 - relative intensity

[b] X-ray pattern obtained from specimen heat treated at 800°C for 23 hrs. Indexing based on monoclinic cell with a = 5.418±0.002Å, b = 9.394±0.001Å, c = 10.765±0.003Å, and β = 99°35±2.4'.

[c] X-ray pattern obtained from specimen heat treated at 1025°C for 20 hrs. Indexing based on cubic cell with a = 8.985±0.001Å.
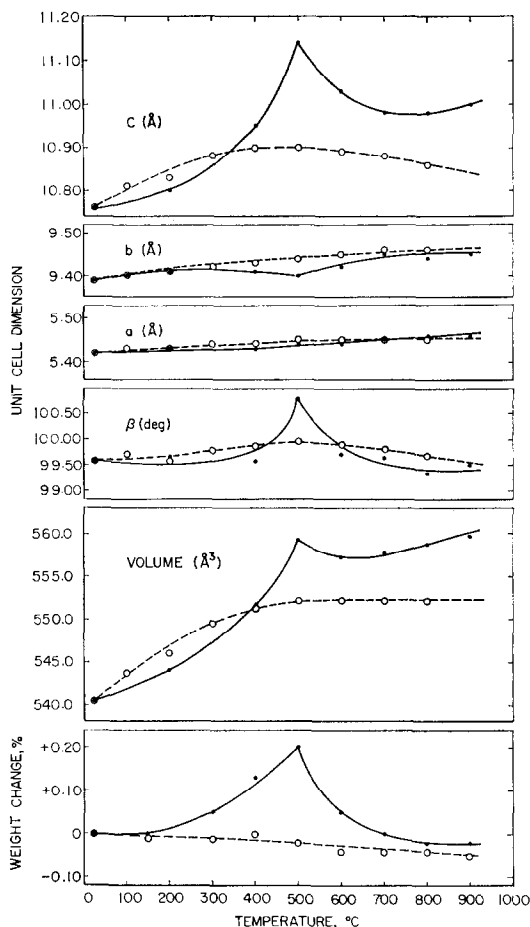
FIG. 2. Unit cell dimensions and weight change versus temperature for $Na_2O \cdot IrO_2$. (●) Data from experiments conducted in an air environment; (○) data from experiments conducted in a helium environment.

Fig. 2. The data were obtained from high-temperature X-ray equipment with the specimen in an air or flowing helium environment. The weight change experiments were conducted on the specimen heated at the indicated temperature for a period of 1 hr, placed in a desiccator and weighed immediately. The room temperature data given in Fig. 2 were obtained from specimens heated at 800°C for 21 hr and quenched in air. The X-ray data indicated well crystallized single-phase material. High-temperature X-ray experiments done in a CO_2 environment gave data similar to those in air, although the X-ray patterns were of poor quality and completely deteriorated at about 600°C. The specimen was examined after cooling and found to have a layer of white amorphous material on the surface.

Perhaps the CO_2 at 1 atm reacted with the 1:1 compound to form the white material which most likely was Na_2CO_3. In air or CO_2, the anomalous behavior of the cell dimensions and weight change suggests a compositional change in the compound. The maximum increase in the unit cell volume, shown in Fig. 2, corresponds to the maximum increase in weight at about 500°C. The phase has probably reacted with CO_2, however O_2 or water vapor can not be precluded. When the 1:1 phase is slowly cooled in air from 800°C, the X-ray pattern shows extra lines, line splitting, and overall poor quality. The nature of the reactions during heating and slow cooling have not been resolved. It is uncertain whether the reaction forms discrete carbonate phases or carbonate solid solutions. Oxide phases ($BaO-NiO-O-CO_2$ system) reacting with atmospheric CO_2 have been reported by Negas and Roth (9) and it appears quite possible the 1:1 phase is reacting likewise. As shown in Fig. 2, the data obtained in a helium environment indicate only thermal expansion. It should be emphasized that the room temperature unit cell dimensions, in Fig. 2, are based on a monoclinic cell and the parameters at the higher temperatures are possibly of a subcell or solid solution.

Table II lists the X-ray powder pattern for the $2Na_2O \cdot 3IrO_2$ (2:3) phase, indexed on the basis of a primitive cubic cell with $a = 8.985$ Å. The dissociation temperature was determined as 1040°C. Various experiments failed to produce a single-phase specimen, residual amounts of the 1:1 and IrO_2 always persisted. The composition of the cubic phase considered most likely is the 2:3 molar ratio. This mixture yielded the greatest quantity of the phase.

3.2. Na_2O-PtO_2 System

The phase diagram for the Na_2O-PtO_2 system in air is given in Fig. 3. The diagram was constructed from the data listed in Table III. The diagram is similar to the Na_2O-IrO_2 system as it also consists of two systems, $Na_2CO_3-Na_2O \cdot PtO_2$ and $Na_2O \cdot PtO_2-PtO_2$. Scheer, VanArkel and Heyding (6) reported that the $Na_2O \cdot PtO_2$ (1:1) compound is isomorphous with the A_2BO_3 series of compounds and proposed cell dimensions based on monoclinic and orthorhombic symmetry. The present study indicates the 1:1 phase is similar in structure with the $Na_2O \cdot IrO_2$ compound. However, the high-temperature X-ray data in air, did not indicate the anomalous behavior of the cell dimensions as was detected

Table III. Experimental Data for Compositions in the Na_2O-PtO_2 System

Composition		Heat Treatment[a]	X-ray Diffraction Analyses[b]	Remarks
Na_2O	PtO_2	Temp. Time		
Mol%	Mol%	°C-hr		
90	10	800-3	$Na_2CO_3+Na_2O\cdot PtO_2$	
		820-1/2		solid
		830-1/2		solid
		835-1/2		solid
		840-1/2	$Na_2CO_3+Na_2O\cdot PtO_2$	solid + liquid
80	20	600-18	$2Na_2O\cdot 3PtO_2+Pt+Na_2CO_3$	nonequilibrium
		700-2	$2Na_2O\cdot 3PtO_2+Na_2CO_3+Na_xPt_3O_4$	nonequilibrium
		700-65	$Na_2O\cdot PtO_2+Na_2CO_3$	
		800-20	$Na_2O\cdot PtO_2+Na_2CO_3$	previous heat treatment 1100-1
		800-192	$Na_2O\cdot PtO_2+Na_2CO_3$	
		1100-1	$Pt+Na_2CO_3$	
66.6	33.3	600-120	$Na_2O\cdot PtO_2+Na_2CO_3$	previous heat treatment 800-20
		600-142	$2Na_2O\cdot 3PtO_2+Na_xPt_3O_4+Na_2CO_3+Pt$	nonequilibrium
		700-21	$Na_xPt_3O_4+Na_2O\cdot PtO_2+2Na_2O\cdot 3PtO_2+Na_2CO_3$	nonequilibrium
		800-20	$Na_2O\cdot PtO_2+Na_2CO_3$	
		900-2	$Pt+Na_2O\cdot PtO_2+Na_2CO_3$	
50	50	600-118	$2Na_2O\cdot 3PtO_2+Na_xPt_3O_4+Pt+Na_2CO_3$	nonequilibrium
		700-19	$Na_xPt_3O_4+Pt+Na_2CO_3+Na_2O\cdot PtO_2$	nonequilibrium
		700-144	$Na_2O\cdot PtO_2$	
		800-20[c]	$Pt+Na_2CO_3$	previous heat treatment 700-1/2
		800-22	$Na_2O\cdot PtO_2$	quenched in liquid nitrogen
		800-71[c]	$Na_2O\cdot PtO_2$	previous heat treatment 800-22
		880-2	$Na_2O\cdot PtO_2$	
		885-2	$Na_2O\cdot PtO_2$	
		890-2	$Na_2O\cdot PtO_2+Pt$	dissociation temperature
		900-2	$Na_2O\cdot PtO_2+Pt$	
		950-17	$Pt+Na_2O\cdot PtO_2$	
		1000-2	$Pt+Na_2O\cdot PtO_2+Na_2CO_3$	nonequilibrium
		1000-21	Pt	
		1100-20	Pt	
40	60	600-43	$2Na_2O\cdot 3PtO_2+Pt$	small amount of Pt
		650-2	$2Na_2O\cdot 3PtO_2+Pt$	
		680-2	$2Na_2O\cdot 3PtO_2+Pt$	
		700-2	$2Na_2O\cdot 3PtO_2+Pt$	
		710-2	$2Na_2O\cdot 3PtO_2+Na_2O\cdot PtO_2+Na_xPt_3O_4$	dissociation temperature
		725-68	$Na_2O\cdot PtO_2+Na_xPt_3O_4+Pt$	nonequilibrium
33.3	66.6	600-118	$2Na_2O\cdot 3PtO_2+Na_xPt_3O_4+Pt$	nonequilibrium
		700-22	$Na_xPt_3O_4+Na_2O\cdot PtO_2+2Na_2O\cdot 3PtO_2$	nonequilibrium
		750-18	$Na_xPt_3O_4+Na_2O\cdot PtO_2+Pt$	nonequilibrium
		800-2	$Pt+Na_2O\cdot PtO_2$	
		800-20	$Pt+Na_2O\cdot PtO_2$	
25	75	600-44	$Pt+Na_xPt_3O_4+2Na_2O\cdot 3PtO_2$	nonequilibrium
		700-23	$Na_xPt_3O_4+Pt+Na_2O\cdot PtO_2$	nonequilibrium
		725-68	$Na_xPt_3O_4+Na_2O\cdot PtO_2+Pt$	trace amount of Pt
20	80	600-96	$Na_xPt_3O_4+Pt+Na_2O\cdot PtO_2$	nonequilibrium
		700-21	$Na_xPt_3O_4+Pt+Na_2O\cdot PtO_2$	nonequilibrium
		700-42	$Na_xPt_3O_4+Pt+Na_2O\cdot PtO_2$	previous heat treatment 700-21
		750-18	$Na_xPt_3O_4+Pt+Na_2O\cdot PtO_2$	nonequilibrium
14	86	500-19	$Pt+Na_2O\cdot PtO_2+Na_xPt_3O_4$	nonequilibrium
		600-19	$Pt+Na_xPt_3O_4+2Na_2O\cdot 3PtO_2$	nonequilibrium
		700-25	$Na_xPt_3O_4+Pt+2Na_2O\cdot 3PtO_2$	trace amount of $2Na_2O\cdot 3PtO_2$
		700-43	$Na_2O\cdot PtO_2+Pt+Na_xPt_3O_4$	previous heat treatment 850-47
		700-552	$Na_xPt_3O_4+Pt$	small amount of Pt
		730-2	$Na_xPt_3O_4+Pt$	
		750-2	$Na_xPt_3O_4+Pt$	
		770-2	$Na_xPt_3O_4+Pt$	
		800-2	$Na_xPt_3O_4+Pt$	
		805-2	$Na_xPt_3O_4+Pt$	
		810-2	$Na_xPt_3O_4+Pt+Na_2O\cdot PtO_2$	dissociation temperature
		850-47	$Pt+Na_2O\cdot PtO_2$	
10	90	600-96	$Na_xPt_3O_4+Pt$	
		700-21	$Na_xPt_3O_4+Pt$	
		700-42	$Na_xPt_3O_4+Pt$	previous heat treatment 700-21
		750-18	$Na_xPt_3O_4+Pt$	
5	95	700-21	$Pt+Na_xPt_3O_4$	
		700-42	$Pt+Na_xPt_3O_4$	previous heat treatment 700-21
		750-18	$Pt+Na_xPt_3O_4$	

[a] All specimens were heat treated in open gold or platinum tubes and air quenched unless otherwise indicated. All temperatures listed applied to (IPTS 1968).

[b] Phases identified are given in order of the relative amount present at room temperature.

[c] Sealed gold tube container; quenched in ice water.

FIG. 3. Phase diagram for the Na$_2$O–PtO$_2$ system in air. (●) Compositions and temperatures of experiments conducted. (1:1) Na$_2$O·PtO$_2$, (2:3) 2Na$_2$O·3PtO$_2$. (····) Metastability; (—·) phase with variable Na content ($0 \leqslant x \leqslant 1$). Polymorphic phase transformations in Na$_2$CO$_3$ (5) were not investigated nor indicated on diagram. Break in base line indicates two systems Na$_2$CO$_3$–Na$_2$O·PtO$_2$ and Na$_2$O·PtO$_2$–PtO$_2$. (?) Composition of vapor and/or liquid phases unknown (see text).

for the Na$_2$O·IrO$_2$ phase. The data for the 1:1 compound in air, indicated only thermal expansion of the cell dimensions. The Na$_2$O·PtO$_2$ X-ray pattern was indexed on the basis of a monoclinic cell, space group $C2/c$, with $a = 5.411$ Å, $b = 9.386$ Å, $c = 10.749$ Å and $\beta = 99°39'$. The dissociation temperature was determined as 890°C. At the dissociation temperature and above, the ? marks shown on the diagram indicate that the equilibrium phases are unknown. The experimental data failed to indicate whether or not the compound melted and if so the composition of the liquid is unknown. It is uncertain if CO$_2$ (absorbed from the air) would exist in the melt as reported in the Na$_2$O–SiO$_2$ system (10). Perhaps the dissociation products are O$_2$, Pt(s) and Na$_2$O(s); the latter would have volatilized and Pt metal would be the only condensed phase.

A recent publication by Urland and Hoppe (11) reported the Na$_2$O·PtO$_2$ compound prepared under an oxygen environment, which is in accord with the present work. Urland and Hoppe (11) also reported a reduced form, Na$_2$PtO$_2$ (orthorhombic symmetry) and a β-Na$_2$O·PtO$_2$ (orthorhombic modification of the monoclinic Li$_2$SnO$_3$-type structure) both prepared under an argon environment. The latter two phases were not detected in the present study and apparently are not stable in air.

The 2Na$_2$O·3PtO$_2$ (2:3) compound appears to be similar to the cubic 2Na$_2$O·3IrO$_2$, although

it forms only on heating indicating, perhaps, that it is metastable in air. The X-ray powder pattern showed broadening of the peaks and overall poor quality. The X-ray pattern was indexed on the basis of a cubic cell with $a = 8.96$ Å. The 2:3 compound dissociates to the 1:1 and Na$_x$Pt$_3$O$_4$ compounds at 710°C.

Waser and McClanahan (12, 13) proposed the crystal structure of Na$_x$Pt$_3$O$_4$ ($0 \leqslant x \leqslant 1$) based on X-ray data obtained from a microcrystalline specimen. Scheer, VanArkel and Heyding (6) also reported the Na$_x$Pt$_3$O$_4$ phase indexed on the basis of a primitive cubic cell with $a = 5.67$ Å. The cell dimensions obtained in the present study are in good accord. There is disagreement among investigators whether the phase contains any sodium at all. Galloni and Busch (14) reported the absence of sodium for the same phase, obtained by the fusion of sodium chloroplatinate with sodium carbonate. This is the same method used by Waser and McClanahan (13). Muller and Roy (15) reported a sodium-free Pt$_3$O$_4$ phase with the Na$_x$Pt$_3$O$_4$-type structure, prepared by heating Pt black for 5 days at 200 atm oxygen and 850°C. During this study various experiments in air, failed to produce the phase (Na$_x$Pt$_3$O$_4$ type structure) in the absence of sodium cations.

Solid solution was not detected in the Na$_x$Pt$_3$O$_4$ phase and the high-temperature X-ray data indicated no unusual behavior at temperatures up to 800°C. Single-phase material was not obtained in this study as residual amounts of Pt

metal always persisted from 0 to 25 mole % sodium. Perhaps the volatility of Na_2CO_3 and grain growth of the Pt black inhibited complete reaction. A composition having the cation ratio 1:3 (Na:Pt) yielded the greatest quantity of the phase.

References

1. C. L. McDANIEL AND S. J. SCHNEIDER, *J. Solid State Chem.* **4**, 275 (1972).
2. C. L. McDANIEL AND S. J. SCHNEIDER, *J. Res. Nat. Bur. Stand., Sect. A* **75**, 185 (1971).
3. C. L. McDANIEL, *J. Amer. Ceram. Soc.* **55**, 426 (1972).
4. T. NEGAS AND R. S. ROTH, *J. Res. Nat. Bur. Stand., Sect. A* **73**, 431 (1969).
5. A. REISMAN, *J. Amer. Chem. Soc.* **81**, 807 (1959).
6. J. J. SCHEER, A. E. VANARKEL, AND R. D. HEYDING, *Can. J. Chem.* **33**, 683 (1955).
7. G. LANG, *Z. Anorg. Allg. Chem.* **276**, 77 (1954).
8. J. F. DORRIAN AND R. E. NEWNHAM, *Mater. Res. Bull.* **4**, 179 (1969).
9. T. NEGAS AND R. S. ROTH, *Nat. Bur. Stand. (U.S.) Spec. Publ.* **364**, 233 (1972).
10. F. C. KRACEK, *J. Amer. Chem. Soc.* **61**, 2869 (1939).
11. V. W. URLAND AND R. HOPPE, *Z. Anorg. Allg. Chem.* **392**, 23 (1972).
12. J. WASER AND E. D. McCLANAHAN, JR., *J. Chem. Phys.* **19**, 413 (1951).
13. J. WASER AND E. D. McCLANAHAN, JR., *J. Chem. Phys.* **20**, 199 (1952).
14. E. E. GALLONI AND R. H. BUSCH, *J. Chem. Phys.* **20**, 198 (1952).
15. O. MULLER AND R. ROY, *J. Less-Common Metals* **16**, 129 (1968).